Effects of soil physical properties on GPR for landmine detection

Timothy W. Miller, Brian Borchers, Jan M.H. Hendrickx, Sung-Ho Hong, Louis W. Dekker, and Coen J. Ritsema

***Abstract*--Field experience has shown that soil conditions can have large effects on Ground Penetrating Radar (GPR) detection of landmines. We discuss available models for the prediction of the dielectric constant from soil physical properties including bulk density, soil texture, and water content. The soil dielectric constant determines the attenuation of the radar signal. The contrast between the dielectric constant of the soil and the landmine is critical in determining the strength of the reflection from the landmine. Field data show considerable spatial variability in soil water content over length scales from centimeters to kilometers. Even under the assumption that other soil properties are homogeneous, the spatial variability of soil water content can lead to large variations in the predicted dielectric constant and resulting GPR response.**

***Index Terms*--Bulk density, dielectric constant, ground penetrating radar, soil texture, spatial variability, soil water content.**

I. Introduction

Field experiments with Ground Penetrating Radar (GPR) and modeling have shown that soil conditions can have a very large effect on the performance of GPR systems for buried landmine detection. Under some soil conditions the landmine signature is of high quality while under others no signature can be detected at all. Fritzsche [1] showed through modeling that GPR signals at 900 MHz would be strongly attenuated in moist soils and in clay soils especially. Trang [2] found in both simulations and actual experiments with a GPR operating in the 600-800 MHz frequency range that it was easier to detect nonmetallic mines when the soil was moist. Johnson and Howard [3] found that the EG&G vehicle mounted GPR system was better able to detect nonmetallic mines at the Energetic Materials Research and Testing Center (New Mexico Tech, Socorro, New Mexico) test site when the soil was relatively moist. Scheers et al. [4] modeled the performance of an ultra wide band GPR operating in the 1-5 GHz range for detection of metallic mines, and found that the maximum depth at which the mine could be detected decreased as the soil moisture increased. Detsch et al. [5] and Koh and Arcone [6] found that signatures from buried metallic mines and nonmetallic mine simulants were stronger in frozen soils than in unfrozen dry soils.

The objectives of this paper are (1) to review a suite of models that can be used for the prediction of soil electrical properties and radar responses under a wide range of soil conditions; (2) to use these models to show the effects that soil physical properties can have on soil electrical properties; (3) to discuss two case studies, one in Socorro, New Mexico and the other in the Netherlands.

Manuscript received February 1, 2002. This work is supported by the Army Research Office (Project 38830-EL-LMD).

T.W. Miller is with the Earth and Environmental Science Department, New Mexico Institute of Mining and Technology, Socorro, NM 87801 USA (e-mail: miller@nmt.edu).

B. Borchers is with the Mathematics Department, New Mexico Institute of Mining and Technology, Socorro, NM 87801 USA (e-mail: borchers@nmt.edu).

J.M.H. Hendrickx is with the Earth and Environmental Science Department, New Mexico Institute of Mining and Technology, Socorro, NM 87801 USA (e-mail: hendrick@nmt.edu).

Sung-Ho Hong is with the Earth and Environmental Science Department, New Mexico Institute of Mining and Technology, Socorro, NM 87801 USA (e-mail: hong@nmt.edu).

L.W. Dekker is with Alterra, Wageningen, The Netherlands.

C. Ritsema is with Alterra, Wageningen, The Netherlands.

II. Models of Soil Electrical Properties and Radar Response

The dielectric properties of a soil depend on a number of factors, including its bulk density, the texture of the soil particles (sand, silt, or clay), the density of the soil particles (typically about 2.6 g/cm^3), the volumetric water content of the soil, the temperature, and the frequencies of interest [7],[8],[9]. Recent research has also shown that the dielectric properties of soil depend on the amount of "bound water" which is in close contact with minerals in the soil [10],[11]. Theoretical and empirical models of the dielectric properties of the different components of the soil have been combined into semiempirical mixing models which can be used to predict the dielectric properties of field soils [7],[10],[11], [12],[13].

In this section we summarize the 1985 model of Dobson, Ulaby, Hallikainen, and El-Rayes [11], and the 1995 model of Peplinski, Ulaby, and Dobson [13]. The earlier model was calibrated for frequencies ranging from 1.4 to 18 GHz [14], and the later was calibrated by fitting the model to a set of experimental observations with a variety of soil textures, soil water contents, and frequencies from 0.3 to 1.3 GHz [13].

The inputs to the 1985 model of Dobson, Ulaby, Hallikainen, and El-Rayes consist of the volumetric soil water content θ, the frequency f, the fraction of sand particles S, the

fraction of clay particles C, the density of the soil particles ρ_S (a typical value is 2.66 g/cm^3), and the bulk density of the soil ρ_B. An empirically derived formula for effective soil conductivity is the following

$$\sigma_{eff} = -1.645 + 1.939\rho_B - 2.013S + 1.594C. \quad (1)$$

The sand and clay fractions also enter the model through two constants which depend on the soil type but are independent of the frequency and soil water content.

$$\beta' = 1.2748 - 0.519S - 0.152C \quad (2)$$

$$\beta'' = 1.33797 - 0.603S - 0.166C \quad (3)$$

The real (ε'_{fw}) and imaginary (ε''_{fw}) parts of the dielectric constant (ε_{fw}) for the free water are given by

$$\varepsilon_{fw} = \varepsilon'_{fw} - \varepsilon''_{fw} i \quad (4)$$

$$\varepsilon'_{fw} = \varepsilon_{w\infty} + \frac{\varepsilon_{w0} - \varepsilon_{w\infty}}{1 + (2\pi f \tau_w)^2} \quad (5)$$

$$\varepsilon''_{fw} = \frac{2\pi f \tau_w (\varepsilon_{w0} - \varepsilon_{w\infty})}{1 + (2\pi f \tau_w)^2} + \frac{\sigma_{eff}}{2\pi\varepsilon_0 f} \frac{(\rho_S - \rho_B)}{\rho_S \theta}. \quad (6)$$

In these formulas, ε_0 is the dielectric permittivity of free space, ε_{w0} is the static dielectric constant of water (80.1 at 20º C), $\varepsilon_{w\infty}$ is the high frequency limit of ε'_{fw} (4.9), and τ_w is the relaxation time of water (9.23x10^{-12} s at 20º C). The dielectric constant of the soil particles (ε_S) is given by the empirical model

$$\varepsilon_S = (1.01 + 0.44\rho_S)^2 - 0.062. \quad (7)$$

Finally, the real (ε') and imaginary (ε'') parts of the dielectric constant for the bulk soil are estimated by

$$\varepsilon = \varepsilon' - \varepsilon'' i \quad (8)$$

where

$$\varepsilon' = \left[1 + \frac{\rho_B}{\rho_S}\left(\varepsilon_S^{\alpha} - 1\right) + \theta^{\beta'} \varepsilon_{fw}'^{\alpha} - \theta\right]^{\frac{1}{\alpha}} \quad (9)$$

and

$$\varepsilon'' = \left[\theta^{\beta''} \varepsilon_{fw}''^{\alpha}\right]^{\frac{1}{\alpha}}. \quad (10)$$

In these formulas, $\alpha = 0.65$ is a constant that has been empirically fitted to experimental data.

The 1995 model of Peplinski, Ulaby, and Dobson which covers a lower frequency range (0.3-1.3 GHz) is identical except the conductivity is given by

$$\sigma_{eff} = 0.0467 + 0.2204\rho_B - 0.4111S - 0.6614C \quad (11)$$

and the real part of the complex dielectric constant is given by

$$\varepsilon' = 1.15\left[1 + \frac{\rho_B}{\rho_S}\left(\varepsilon_S^{\alpha} - 1\right) + \theta^{\beta'} \varepsilon_{fw}'^{\alpha} - \theta\right]^{\frac{1}{\alpha}} - 0.68. \quad (12)$$

As GPR signals travel through the soil, they are attenuated at a rate determined by the complex dielectric constant of the soil. The one way attenuation loss in db/m is given by

$$\text{Attenuation Loss} = 8.6855 d\alpha \quad (13)$$

where d is the depth to the object from which the GPR signal is reflecting, and α is given by

$$\alpha = \frac{2\pi f}{c} \sqrt{\left(\frac{\varepsilon'_S}{2}\left(\sqrt{1 + \left(\frac{\varepsilon''_S}{\varepsilon'_S}\right)^2} - 1\right)\right)} \quad (14)$$

where c is the speed of light 2.997x10^8 m/s.

Another important factor in determining the performance of GPR systems is the strength of the reflection from the landmine surface. Often in geophysical studies the reflection from a subsurface layer is calculated using simple plane wave reflection theory. In this theory the reflection coefficient is calculated by taking the difference of the square roots of each dielectric layer and dividing it by the sum of the square roots of each dielectric layer. For this to be accurate, the reflecting subsurface layer must be very large in comparison to the wavelength of the electromagnetic wave. However, when the reflecting layer is a landmine the wavelength of the electromagnetic wave may be very close to the diameter of the landmine and plane wave reflection theory should not be used.

Although this is the case, a qualitative discussion of the reflection coefficient from metallic and nonmetallic mines is in order. Plastic landmines usually have dielectric constants that are low, very close to the dielectric constant of dry soil, where metallic landmines have dielectric constants that approach infinity since they are conductors. So metallic landmines will produce perfect reflections under all soil conditions where nonmetallic landmines will produce reflections governed by the contrast in the dielectric constant of the soil and the landmine.

III. Model Predictions

The mathematical models described here have been integrated into a MATLAB package, which can be found online at http://www.nmt.edu/~borchers/dielectrics.html. In this section the soil properties of two field soils from the Socorro, New Mexico area are used in the MATLAB program to demonstrate the effects that soil physical properties can have on soil electrical properties. The soil physical properties were measured at New Mexico Tech and include the following: bulk density, sand, silt, and clay distributions. The particle density was assumed to be 2.66 g/cm^3. For a complete description of the soil physical properties of both soils refer to Section 3.1.

A. Dielectric constant and soil water content

Figures 1 and 2 show how the complex dielectric constant changes with soil water content for the two soils. In both of these soils the real part of the dielectric constant increases with soil water content, where the imaginary part remains almost constant over the entire range of soil water contents.

Relating this to landmine detection, if a nonporous plastic landmine is buried in a sand or clay soil, then as the soil water content increases, the bulk dielectric constant of the soil also increases, while the dielectric constant of the landmine remains the same (about 3-4). This elevation in dielectric constant of the soil will lead to a larger reflection coefficient (approaching unity), which in theory will lead to better detection of the landmine.

Figure 1 predicts that the real part of the dielectric constant will be 27 for the sand soil at 27% volumetric soil water content, and Figure 2 predicts a value of 23 for the real part of the dielectric constant of the clay soil at 36% volumetric soil water content. If the bulk dielectric constant and soil water content are the only factors examined when detecting nonmetallic landmines, one may come to the erroneous conclusion that for all soils landmine detection will improve with increasing soil water content because the dielectric constant contrast increases with elevated soil water contents.

B. Dielectric constant and frequency

The bulk dielectric constant of a soil will also change depending on the frequency of the GPR system. Figures 3 and 4 show how the complex dielectric constant varies with frequency for the same soils at saturated soil water conditions. The gaps seen in the dielectric constant between the lower and higher frequencies (1.3 to 1.4 GHz) are caused because of patching the high and low frequency models together. These two models are only approximations and because of this they do not produce consistent results at their higher and lower frequency ends, respectively. In Figure 3, over the 0.3 to 1.3 GHz range, the imaginary part of the dielectric constant for sand is basically invariant and does not contribute a significant influence to the overall complex dielectric constant.

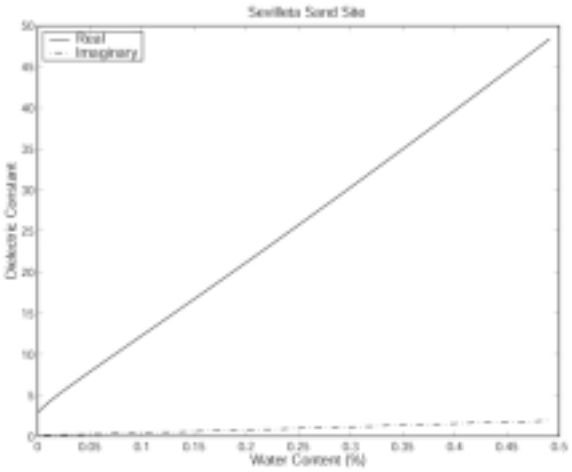

Figure 1 Plot of dielectric constant vs. soil water content for Sevilleta sand at 900 MHz.

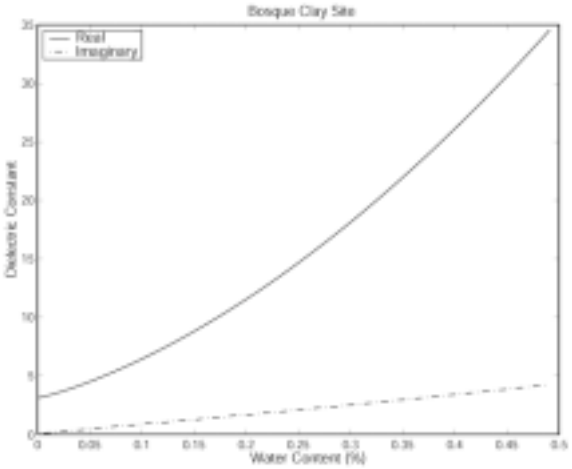

Figure 2 Plot of dielectric constant vs. soil water content for Bosque Del Apache clay at 900 MHz.

For the clay soil over that same range (See Figure 4) the imaginary part or loss term is extremely significant. Over the high frequency range (1.4 to 6 GHz), the imaginary part of the dielectric constant increases for both the sand and clay soils. Thus, from figures 3 and 4, it is clear that the frequency of the GPR system can cause the bulk dielectric constant of the soil to either increase or a decrease depending on the frequency range. Furthermore, soil texture plays a significant role in the lower frequency range (0.3 to 1.3 GHz) as seen in the clay soil.

C. Dielectric constant and soil bulk density

Along with frequency and water content, the complex dielectric constant will change slightly with variations in the bulk density of a soil. Figure 5 is a plot of the complex dielectric constant of the Sevilleta sand soil versus the bulk density, using 900 MHz and 27% volumetric soil water content as inputs in the model. The real part of the dielectric constant shows a slight increase at higher bulk densities while the imaginary part shows little change as the bulk density is varied from 1.5 to 1.9 g/cm^3. The same is true for the

complex dielectric constant in the Bosque clay soil (See Figure 6) with the exception of the slight decrease in the imaginary part at higher bulk densities.

D. Dielectric constant and soil particle density

Soil particle density will also show a slight effect on the complex dielectric constant of sand and clay soils. Both figures 7 and 8 are plots showing the relation between particle density and dielectric constant for the Sevilleta sand and the Bosque clay soil at 900 MHz and saturated soil water contents. For these figures the complex dielectric constant is invariant over the 2.25 to 2.75 g/cm^3 range, with the slight exception of the imaginary part of the Bosque clay soil showing some increase at higher frequencies. Figures 5 through 8 illustrate that bulk soil density and the particle density contribute very little to the over all complex dielectric constant when the soil is saturated. This is also true at lower water contents.

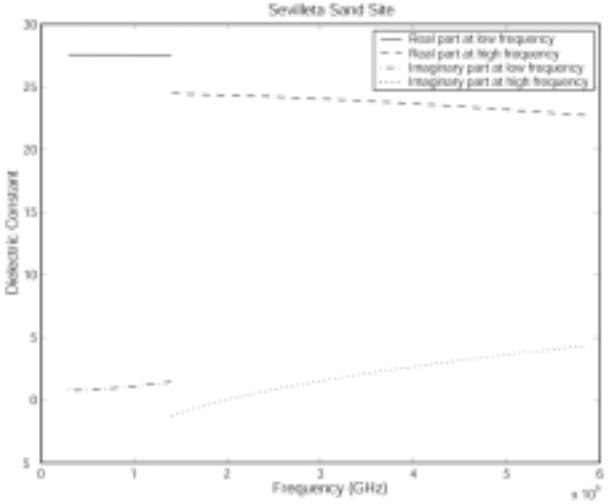

Figure 3 A plot of dielectric constant vs. frequency for Sevilleta sand at 27% volumetric soil water content.

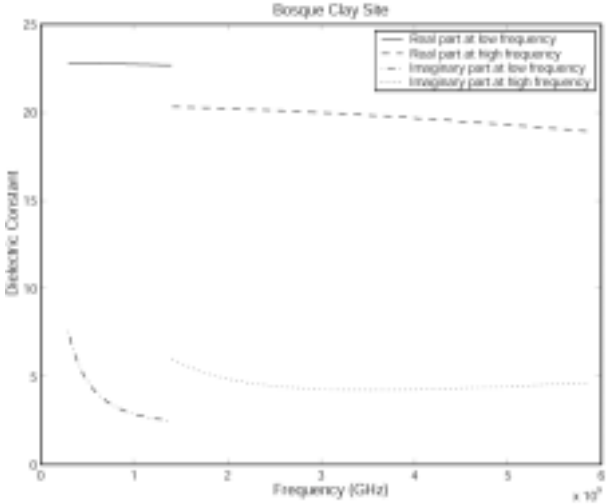

Figure 4 A plot of dielectric constant vs. frequency for Bosque Del Apache clay at 36% volumetric soil water content.

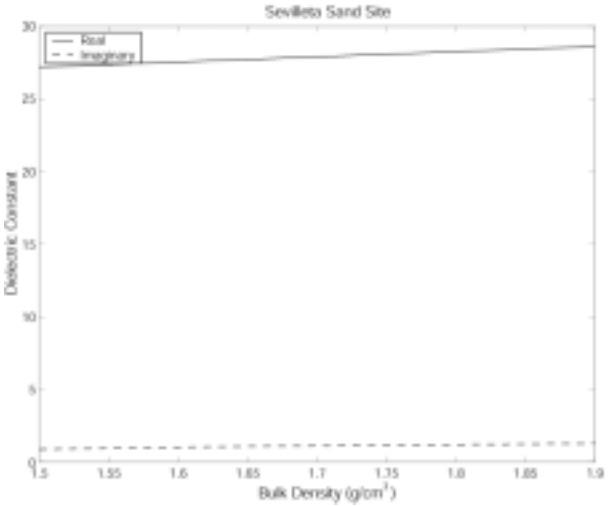

Figure 5 A plot showing the relationship between bulk density and the dielectric constant for the Sevilleta sand soil at 900 MHz and 27% volumetric soil water content.

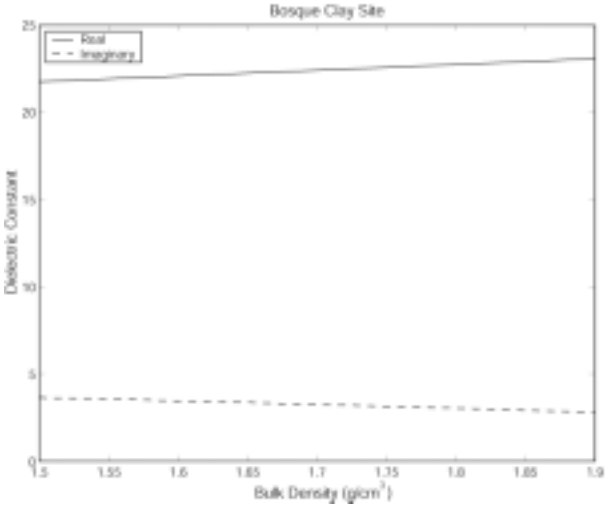

Figure 6 A plot showing the relationship between bulk density and the dielectric constant for the Bosque clay soil at 900 MHz and 36% volumetric water content.

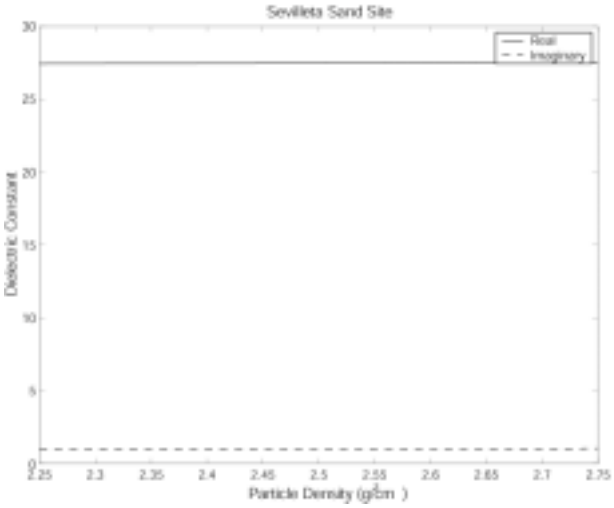

Figure 7 A plot showing the relationship between particle density the and dielectric constant for the Sevilleta sand soil at 900 MHz and 27% volumetric soil water content.

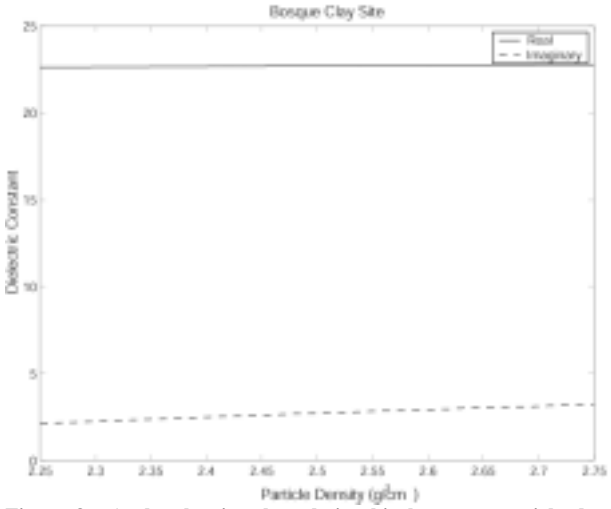

Figure 8 A plot showing the relationship between particle density and the dielectric constant for the Bosque clay soil at 900 MHz and 36% volumetric water content.

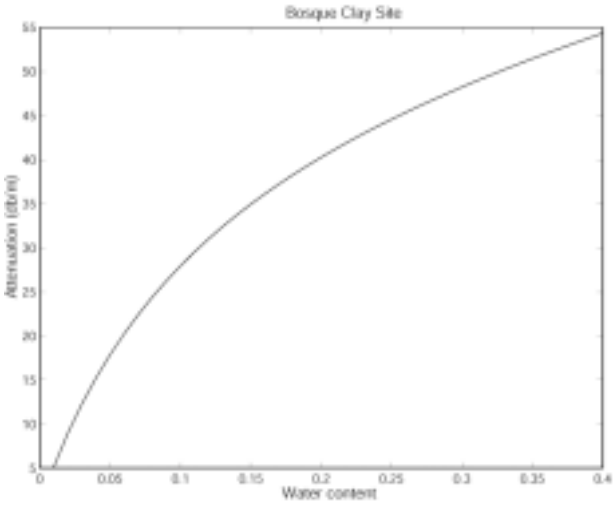

Figure 10 Plot of attenuation vs. soil water content for Bosque Del Apache clay soil at 900 MHz.

E. Attenuation and radar response

From Equation 14 it is clear that radar wave attenuation should increase with frequency and dielectric constant as the soil water content increases. In figures 9 and 10 the attenuation that corresponds with a range of soil water contents have been plotted for both soils. From these two figures it is obvious that clay soils have a larger amount of attenuation at saturated soil water contents than sand soils at similar water content.

Figures 11 and 12 show how changes in frequency relate to radar wave attenuation. As frequency increases, the attenuation of the GPR signal in both clay and sand soils increases rapidly. The break in the plots between 1.3 and 1.4 GHz is for the same reason as explained before. High frequency radar is often used to enhance resolution since resolution increases with frequency, but as shown in these figures signal attenuation increases quite dramatically at higher frequencies for sand and clay soils.

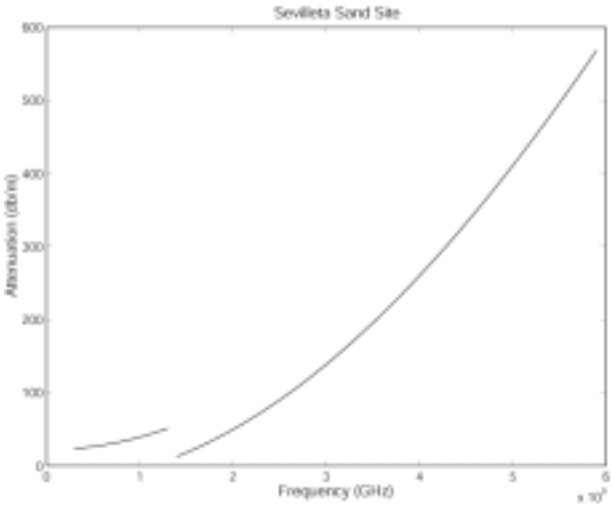

Figure 11 Plot of attenuation vs. frequency for the Sevilleta sand soil at 27% volumetric soil water content.

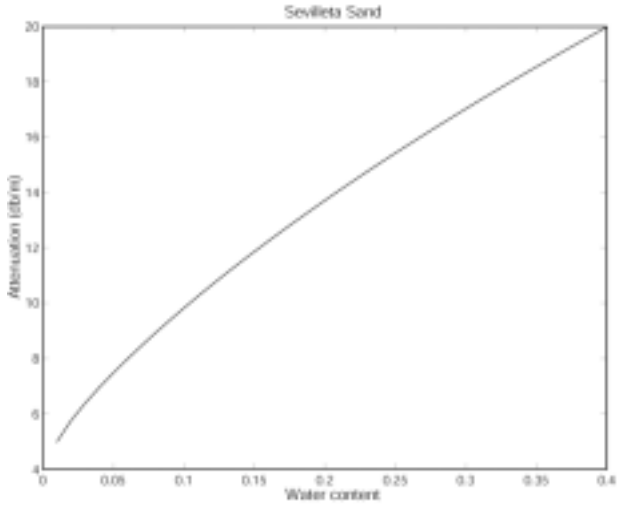

Figure 9 Plot of attenuation vs. soil water content for Sevilleta sand soil at 900 MHz.

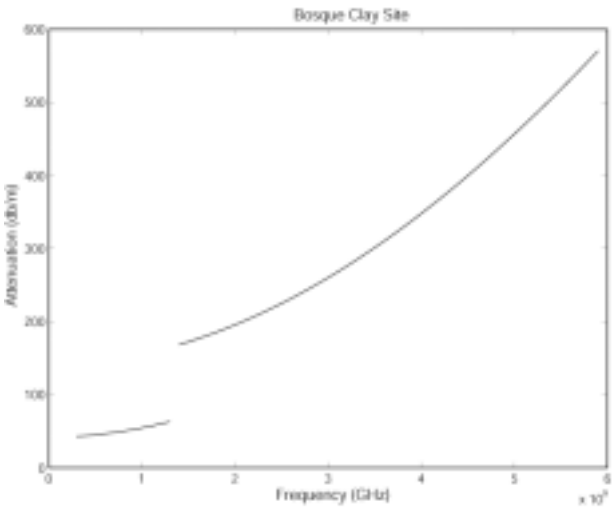

Figure 12 Plot of attenuation vs. frequency for the Bosque Del Apache clay soil at 36% volumetric soil water content.

IV. Case Study 1: Application of Water to Field Soils

A. Study sites

To demonstrate the effect of applying water to enhance the bulk dielectric constant of field soils, we describe two experiments. One was performed at the Sevilleta National Wildlife Refuge and the other at the Bosque Del Apache Wildlife Refuge, both located near Socorro, New Mexico. The soil at the Sevilleta site is a dry sandy soil, with a typical soil water content of 5% and a soil texture of 95% sand, 2% silt, and 3% clay. The bulk density of the soil is approximately 1.6 g/cm^3. The soil at the Bosque site is a clay soil, with an average soil water content range of approximately 4% to 45% depending on the time of year. It has a soil texture of 1.3% sand, 26.5% silt, and 72.2% clay. The bulk density of the soil is approximately 1.8 g/cm^3. The soil texture and bulk density of these samples were determined using standard methods [15], [16].

B. Equipment

The simulant landmines used in this experiment were completely inert and are composed of Dow Corning 3110 RTV Silicon Rubber. The TNO Physics and Electronics Laboratory in the Netherlands, which specializes in producing inert landmines for detection purposes, manufactured the landmines. For imaging the simulant landmines we used a Ground Penetrating Radar (pulseEKKO 1000) system, which is manufactured by Sensors and Software Ltd, Canada. We chose their 900 MHz antenna configuration that has an antenna separation of 17 cm. For data collection, we conducted a reflection survey with a step size of 2.0 cm, 64 stacks per trace, Automatic Gain Control (AGC), and we set our trace correction to DEWOW. These parameters provided enough spatial resolution to locate the simulant landmines under most of the field conditions encountered.

C. Experiment

For both of the sites listed in Section 3.1 we chose a 2 meters by 2 meters study area. Inside the study areas we constructed a wooden frame with dimensions of 1 meter by 2 meters. The frame was used to house the target landmine and provided a reference frame for the Ground Penetrating Radar system. The target landmine was buried inside the frame area and its location was recorded.

For the sand site we placed the target landmine 60 cm from the end and 50 cm from the side of the frame and buried it 11 cm below the ground surface. For the clay site, the target landmine was also buried 11 cm deep, but it was positioned 100 cm from the end and 50 cm from the side of the frame. We also placed a second landmine outside the wooden frame, which was used to observe soil water content. The soil water content was recorded using TDR probes [15] that were placed around this second landmine. There were 4 TDR probes in total that were buried 3, 8, 23, and 28 cm below the ground surface. To apply water to the sites we used a sprinkler system for the sand site and "ponding" for the clay site. Before and after the application of water we measured the volumetric soil water content with the TDR probes and collected GPR data. The raw radar signals were then analyzed using software from Sensors & Software Ltd, Canada.

D. Results

In this section we present wiggle trace plots of the unprocessed GPR traces. Figure 13 shows two GPR wiggle trace plots for the Sevilleta sand site. Plot (A) in this figure was imaged under normal field conditions (10% volumetric soil water content), and plot (B) was imaged after raising the volumetric soil water content to 27%. The landmine in this figure is indicated by the hyperbolic feature directly below the 0.5 meter mark on the horizontal scale. These plots clearly show that raising the volumetric soil water content of dry sandy soils can enhance the ability of the GPR to image landmines.

However, applying water to very dry clay soils does not appear to enhance detection. Figure 14 shows wiggle trace plots from the Bosque Del Apache clay site. Plot (A) in Figure 14 is an image taken during dry field conditions (4% volumetric soil water content), and plot (B) is an image from the same site after applying 2700 liters of water (raising the volumetric soil water content to 36%). The landmine is detected under the dry clay soil conditions shown in plot (A). The landmine in this figure is also shown by the hyperbolic feature directly below the 0.63 meter mark on the horizontal scale. This detection is not as clear as in Figure 13 due to the low contrast in dielectric constant between the landmine and the surrounding dry clay soil.

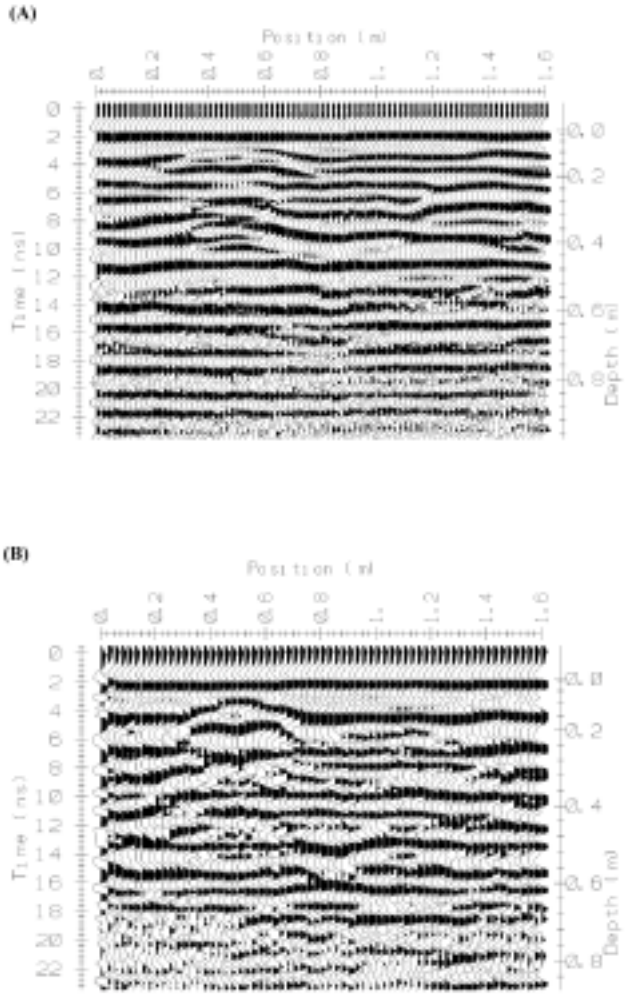

Figure 13 Sevilleta sand soil, 10% volumetric soil water content (A), and 27% volumetric soil water content (B).

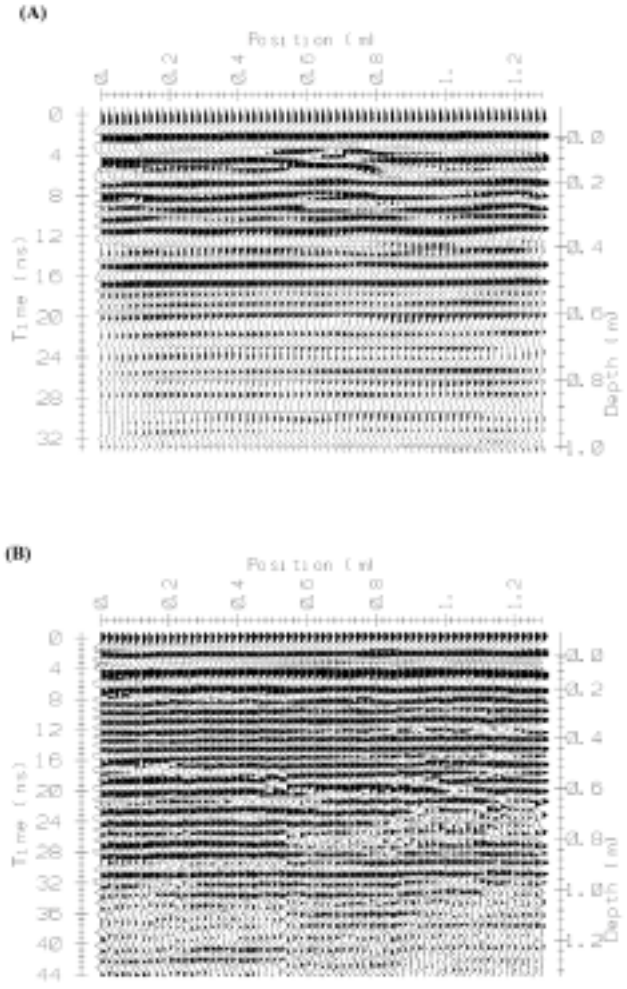

Figure 14 Bosque Del Apache clay soil, 4% volumetric soil water content (A), and 36% volumetric soil water content.

After application of water (See plot (B) of Figure 14) the landmine is clearly invisible to GPR. This is expected because in clay soils the electrical conductivity is high and adding water greatly increases the attenuation of the radar signal.

To check our model against the field experiments, the dielectric constant was calculated for each soil with the model and then from the raw GPR traces. The dielectric constant from the model was calculated using the equations explained in Section II. The dielectric constant from the experimental data was calculated from the raw traces (Figures 13 and 14) by picking the travel time from the trace that corresponded with the top of the landmine. This time was then used with the depth of burial to calculate the velocity of the soil under the specific soil water content. The dielectric constant was then calculated by squaring the ratio of the speed of light to the velocity of soil. The dielectric constants from the experimental work came within 10% of what our model predicted.

V. Case Study 2: Spatial variability of soil water content

In previous modeling studies [17], it was assumed that our soils were homogeneous throughout, i.e. the variability of soil water content is caused only by temporal variability of weather parameters such as precipitation and evaporation or by the affect of the mine on water distribution. However, many field observations have shown that soil water content has its own intrinsic spatial variability due to small differences in hydraulic properties, surface unevenness, vegetation, unstable wetting, and macropore flow [18], [19], [20], [21].

We will now present an example of the spatial variability of soil water content in a water repellent soil in the Netherlands to infer how soil water content variability affects the variability of dielectric soil properties and the performance of a GPR for mine detection.

A. Water Repellent Soil in the Netherlands

This field experiment was carried out by Ritsema and Dekker [22] in the western part of the Netherlands near the village of Ouddorp. Between April 1988 and March 1989, ten 5.5 m long and 0.5 m deep trenches were sampled in a 0.05 ha experimental field. For each transect, 100 samples (diameter 5 cm; height 5 cm; volume 100 cm^3) were collected at depths of 5-10, 15-20, 25-30, 35-40 and 45-50 cm. Over the entire study, a total of 5000 soil samples were collected. Each sample was used to determine volumetric soil water content and the degree of actual water repellency. Precipitation and ground water depths in the field were measured weekly. A total precipitation of 645 mm was measured between the first and last sampling campaigns. The ground water depth fluctuated between 70 cm and 155 cm below the soil surface. For more details we refer to Ritsema and Dekker [22].

The soil texture consisted of 97% sand and 3% clay. The organic matter content of the top 5 cm was 8.9%, from 5-15 cm organic matter content was approximately 1%, and below 15 cm it was around 0.5% [23].

For each of the sampling locations near Ouddorp, the mean volumetric water content and the coefficient of variability were calculated for each measurement day. In addition, the statistical distribution of the data was determined. Sufficient data were available concerning the water repellent soil in the Netherlands for the calculation of semivariograms to determine the spatial correlation length of soil water content.

The coefficients of variability for this soil varies from about 5% to as high as 83% with a typical value of 10% to 30%. The highest coefficients of variability observed coincided with increased actual field measured water repellency [22]. Because water repellency leads to unstable wetting fronts [24], a high soil water content variability is expected. Since water repellency occurs in surface soil layers all over the world (e.g,. [25]), these high coefficients of variability seem to be the norm rather than the exception.

Figure 15 shows the variations of soil water content with depth in the first transect from the Netherlands. Within each depth range, the soil water contents are approximately normally distributed. Furthermore, the standard deviation increases with mean water content. The coefficient of variability ranges from about 10% to 20%. Note the systematic trends in soil water content with depth. Similar patterns were observed in the other nine transects. In general, we can expect that water content will vary systematically with depth, with random variation within each depth layer. The depth profile of water contents is determined largely by the dynamics of wetting and drying fronts passing through the soil. Thus, geostatistical analysis of the variation with depth is not appropriate.

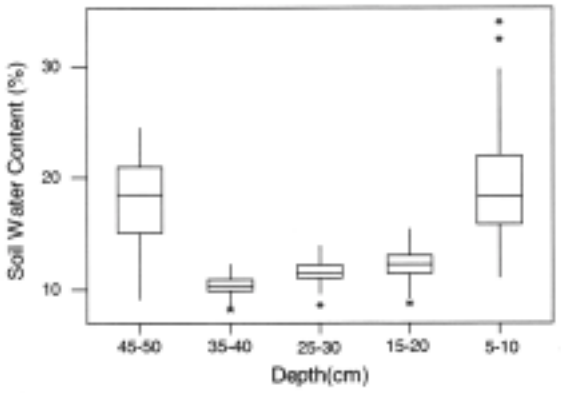

Figure 15 Variation of soil water content with depth for the first Netherlands transect.

However, geostatistical analysis of the random variation within layers is appropriate. Figure 16 shows an empirical semivariogram for the soil water content in the 5-10 cm layer of the first transect. We would expect to see some spatial correlation of soil water content. The semivariogram shows that the spatial correlation length is 40 cm or less. Similar results were obtained for the other layers within the first transect and for the other nine transects. The spatial correlation lengths ranged from about 10 cm to 50 cm. For this water repellent soil, there is very little spatial correlation, resulting in a highly random distribution of soil water content.

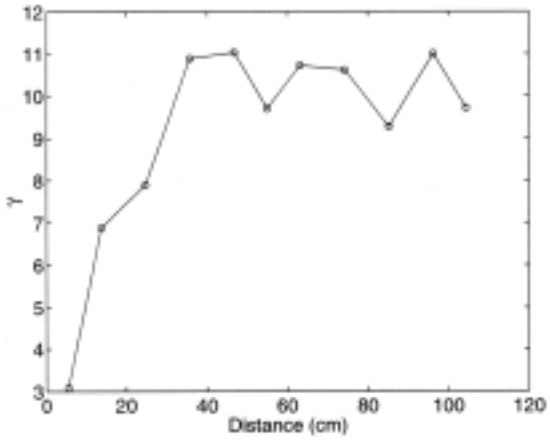

Figure 16 Semivariogram of soil water content for the first layer of the first transect of the Netherlands data.

B. Response of Ground Penetrating Radar

When there is uncertainty in soil water content, there will also be substantial uncertainty in the strength of GPR reflections, because of the varying attenuation losses and because of variations in the strength of the reflection from the landmine. For example, consider a GPR survey in a minefield. If the soil has not been altered by applying water, then it will naturally contain areas with high and low soil water content. The attenuation of the GPR over a transect in

this minefield will vary as the soil water content varies spatially. Furthermore, dielectric constant has been shown to vary substantially with soil water content. If there are naturally occurring dry pockets in the soil, on the order of the size of landmines, then a false detection may be produced if the contrast between the dry pocket and the surround soil is large enough.

VI. Conclusions

In this study we have measured the soil physical properties (texture, water content, bulk density) of a sand and clay soil in the field. The measured values have been used for the prediction of soil electrical properties using models from the literature. Soil water content has the largest effect on the dielectric constant: in both soils the real part of the dielectric constant increases more than one order of magnitude when soil water content increases from zero to saturation. The effects of soil bulk density and soil particle density on dielectric constant are minor.

We also evaluated the effect of radar frequency on the soil dielectric constant. Soil texture clearly interacts with the frequency: in sand the dielectric constant changes little with frequency while in clay in the range 0.3-1.3 GHz the dielectric constant show a sudden decrease from 7 to 3. Although not very large this decrease may be important for the detection of mines in dry clay soils since mines have a dielectric constant of approximately 3 to 4. The frequency effects are one order of magnitude less than those of changes in soil water content which makes the latter factor the most determinant for use of GPR for mine detection.

The attenuation of the radar signal in the soil depends strongly on both soil water content and soil texture. For both soils the attenuation at 900 MHz increases one order of magnitude with increasing soil water content from dry to saturation. The increase in the clay soil is twice as large as in the sand soil. The attenuation also depends strongly on the frequency; it increases with about one order of magnitude when the frequency increases from about 1 to 8 GHz.

Based on our evaluation of the models we predict that an increase in soil water content in the sand soil will lead to a stronger landmine signature. In a clay soil, however, due to an increased attenuation at higher soil water contents, we predict the land mine signature to be much weaker. These predictions have been verified with field measurements. Thus, the semiempirical radar models can be used for the evaluation of radar signals under different soil conditions.

Since soil water constant is such a dominant factor for radar response, we explored its spatial variability in field soils. Literature reports and our case study from the Netherlands indicate that soil water content in soil surface layers is highly variable. Not only are there systematic changes due to weather conditions but there is also a highly random component. The high variability of soil water content will lead to a high variability of dielectric constants.

Knowledge of soil texture and soil water content variability and how these affect soil electrical properties of the soil is essential for the effective development and deployment of Ground Penetrating Radar systems for mine clearance operations.

VII. References

[1] Fritzsche, M. 1995. Detection of buried landmines using ground penetrating radar. Proceedings of the SPIE 2496, pp. 100-109.

[2] Trang, A.H. 1996. Simulation of mine detection over dry soil, snow, ice, and water. Proceedings of the SPIE 2765, pp. 430-440.

[3] Johnson, P.G., and P. Howard. 1999. Performance results of the EG&G vehicle mounted mine detector. Proceedings of the SPIE 3710, pp. 1149-1159.

[4] Scheers, B., M. Acheroy, and A. Vander Vorst. 2000. Time domain modeling of UWB GPR and its application on landmine detection. Proceedings of the SPIE 4038, pp. 1452-1460.

[5] Detsch, R.M., T. F. Jenkins, S. A. Arcone, G. Koh, and K. O'Neil. 1998. Environmental effects on detection of buried mines and UXO. Proceedings of the SPIE 3392, pp. 1261-1264.

[6] Koh, G., and S.A. Arcone. 1999. Radar detection of simulant mines buried in frozen ground. Proceedings of the SPIE 3710, pp. 749-755.

[7] P. Hoekstra and A. Delaney, "Dielectric properties of soils at UHF and microwave frequencies," *J. of Geophysical Res.,* **79**, pp. 1699-1708, 1974.

[8] G. C. Topp, J. L. Davis, and A. P. Annan, "Electromagnetic determination of soil water content: measurements in coaxial transmission lines," *Water Resour. Res.,* **16**, pp. 574-582, 1980.

[9] F. T. Ulaby, R. K. Moore, and A. K. Fung, *Microwave remote sensing : active and passive, volume 3*, Artech House, Dedham, MA, 1986.

[10] J. R. Wang and T. J. Schmugge,. "An empirical model for the complex dielectric permittivity of soils as a function of water content," *IEEE Trans. Geosci. Remote Sens.*, **18**, pp. 288-295, 1980.

[11] M. C. Dobson, F. T. Ulaby, M. T. Hallikainen, and M. A. El-Rayes, "Microwave dielectric behavior of wet soil - Part II: Dielectric mixing models," *IEEE Trans. Geosci. Remote Sens.*, **23**, pp. 35-46, 1985.

[12] D. Wobschall, "A theory of the complex dielectric permittivity of soil containing water, the semidisperse model," *IEEE Trans. Geosci. Electron.,* **15**, pp. 49-58, 1977.

[13] N. R. Peplinski, F. T. Ulaby, and M. C. Dobson, "Dielectric properties of soils in the 0.3-1.3GHz range," *IEEE Trans. Geosci. Remote Sens.*, **33**, pp. 803-807, 1995.

[14] M. T. Hallikainen, F. T. Ulaby, M. C. Dobson, and M. A. El-Rayes, "Microwave dielectric behavior of wet soil - Part I: Empirical models and experimental observations," *IEEE Trans. Geosci. Remote Sens*., **23**, pp. 25-34, 1985.

[15] J. M. H. Hendrickx, "Determination of hydraulic soil properties," in *Process studies in hillslope hydrology*, M. G. Anderson and T.P. Burt eds.,. pp. 43-92, Wiley, New York, 1990.

[16] A. Klute ed., *Methods of Soil Analysis - Part 1 Physical and Mineralogical Methods (Second Edition),* Agronomy Monograph No. 9., SSSA, Madison, WI, 1986.

[17] B. Borchers, J. M. H. Hendrickx, and B. S. Das, "Modeling Distributions of Water and Dielectric Constants Around Landmines in Homogeneous Soils," in *Detection and Remediation Technologies for Mines and Minelike Targets IV,* A. C. Dubey, J. F. Harvey, J. T. Broach and R. E. Dugan eds. Proceedings of SPIE [3710-70], pp. 728_738, SPIE, Bellingham, WA, 1999.

[18] Hendrickx, J.M.H., Wierenga, P.J. & Nash, M.S. "Variability of soil water tension and soil water content." *Agricultural Water Management*, 18; 135-148. 1990.

[19] Hendrickx, J. M. H. and G. Walker, "Recharge from precipitation", Chapter 2, In: I. Simmers (ed.), Recharge of phreatic aquifers in (semi)-arid areas, Balkema, Rotterdam, The Netherlands, 1997.

[20] Nielsen, D.R., J.W. Biggar, and K.T. Ehr. "Spatial variability of field-measured soil-water properties." *Hilgardia* 42:215-259. 1973.

[21] Peck, A.J. "Field variability of soil physical processes." In: D.I. Hillel (Ed.), *Advances in Irrigation*, Vol. 2, Academic Press, New York. 1983.

[22] Ritsema, C.J. and L.W. Dekker, "How water moves in a water repellent sandy soil 2. Dynamics of fingered flow," *Water Resour. Res.*, **30**. pp. 2519-2531. 1994.

[23] Dekker, L.W. Moisture variability resulting from water repellency in Dutch soils. Doctoral thesis, Wageningen Agricultural University, The Netherlands, 240 pp. 1998.

[24] Hendrickx, J.M.H., Dekker, L.W. & Boersma, O.H. "Unstable wetting fronts in water repellent field soils." *J. Environ. Qual.,* 22; 109-118. 1993.

[25] Jaramillo, D. F., L. W. Dekker, C. J. Ritsema, and J. M. H. Hendrickx, "Occurrence of soil water repellency in arid and humid climates." *J. of Hydrology*, 231/232,105-114, 2000.